EurJOC European Journal of Organic Chemistry

FULL PAPER

DOI: 10.1002/ejoc.201403457

# Elucidating the Structural Isomerism of Fluorescent Strigolactone Analogue CISA-1

Hannelore Goossens,[a] Thomas S. A. Heugebaert,[b] Busra Dereli,[c][‡] Melissa Van Overtveldt,[b] Ozlem Karahan,[c] Ilknur Dogan,[c] Michel Waroquier,[a] Veronique Van Speybroeck,[a] Viktorya Aviyente,[c] Saron Catak,*[a,c] and Christian V. Stevens*[b]

**Keywords:** Atropisomerism / Lactones / Conformation analysis / Configuration determination / Density functional calculations

The synthesis of a new potent strigolactone analogue (CISA-1), resulting in the formation of two interconverting structural isomers, which could not be identified, was recently reported. In the present study, a combined computational and experimental approach is used to identify the exact nature of these structural isomers. Although standard experimental techniques could not be used to determine the identity of the isomers, chromatographic methods excluded *E*/*Z* isomerisation. Computational $^1$H NMR chemical shift values and DFT calculations on interconversion barriers strongly suggest that the CISA-1 isomers were interconverting (*Z*)-configured atropisomers.

## Introduction

Since the first report of (+)-strigol (**1**; Figure 1) in the late 1960s,[1] strigolactones (SLs) have gradually emerged as a new class of plant hormones. In the last five years, their involvement in a myriad of processes and pathways was proven, ranging from node elongation to fungal symbiosis. This large variety of biological functions has resulted in an exponentially increasing number of research papers discussing strigolactones.[2]

Hampered by the inaccessibility of naturally occurring strigolactones (only picogram amounts per day are produced per plant[3]) and their structural complexity, most of the published research is based on genetic techniques and the use of synthetic, simplified SL analogues, of which GR24 (**2**; Figure 1) is the most prominent example.[4] As such, potent SL analogues are one of the two pillars upon which strigolactone research is built.

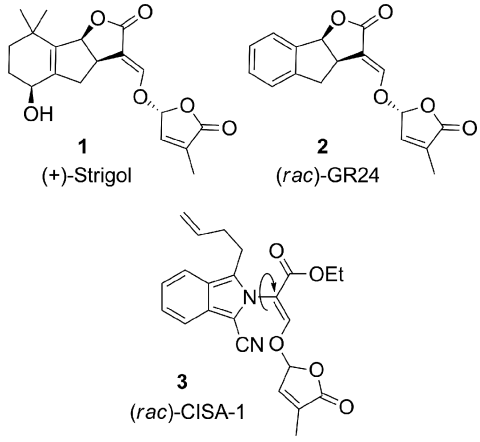


Figure 1. (+)-Strigol and its synthetic analogues GR24 and CISA-1.

Recently, we have described the synthesis and bioactivity of CISA-1 (**3**; Figure 1), a fluorescent alternative to GR24.[5] This compound proved to be more effective at inhibiting adventitious rooting and at stimulating *Orobanche* germination compared with the widely used GR24. For several other parasitic species, potent germination induction was observed, but CISA-1 did not perform as well as GR24. For branching inhibition, the two strigolactone analogues were equally effective in both *Arabidopsis* and pea. Furthermore, we have shown the absence of phytotoxicity. In addition, CISA-1 showed activity in arbuscular mycorrhizal (AM) fungal branching, albeit moderate.[6]

The synthesis of CISA-1 proceeds through the classical pathway of O-alkylation of formyl ester **4** (Scheme 1). How-

[a] Center for Molecular Modeling, Ghent University, Technologiepark 903, 9052 Zwijnaarde, Belgium
molmod.ugent.be
[b] Research Group SynBioC, Department of Sustainable Organic Chemistry and Technology, Faculty of Bioscience Engineering, Ghent University,
Coupure links 653, 9000 Ghent, Belgium
E-mail: Chris.Stevens@UGent.be
http://www.ugent.be/bw/doct/en/research-groups/synbioc
[c] Department of Chemistry, Bogazici University, 34342 Bebek, Istanbul, Turkey
E-mail: Saron.Catak@boun.edu.tr
http://www.ccbg.chem.boun.edu.tr
[‡] Current address: Department of Chemistry, University of Minnesota,
207 Pleasant St. SE, Minneapolis, MN 55455-0431, USA
Supporting information for this article is available on the WWW under http://dx.doi.org/10.1002/ejoc.201403457.

  

ever, in contrast to all other reports describing strigolactone syntheses, this resulted in the formation of two structural isomers. The exact nature of these isomers has not yet been determined. In the original report by Rasmussen et al.[5a], a suggestion was made about the importance of rotation about the C–N bond (as shown in Figure 1) with formation of rotamers. In this paper, all experimental data on the topic will be investigated in detail and theoretical calculations will be performed to finally reveal the occurrence of (*E*)- or (*Z*)-isomers and their interconversion.

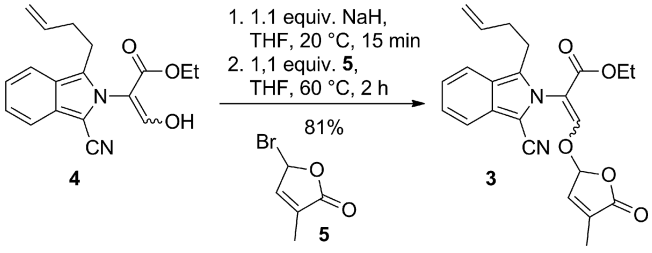


Scheme 1. Final step of the synthesis of CISA-1.[5]

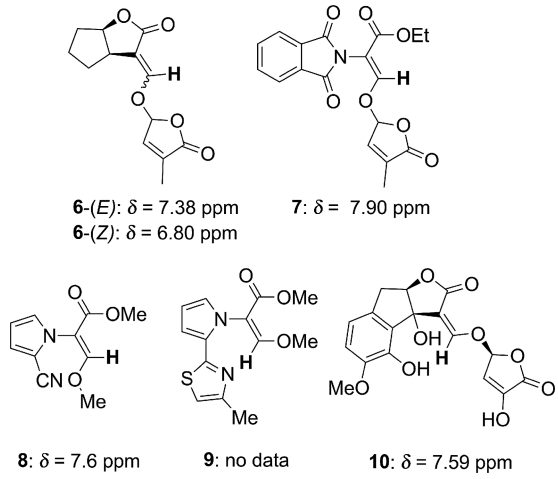


Figure 2. Closest reported examples of (*E*)- and (*Z*)-configured enol ethers.[12,13]

## Results and Discussion

### Attempted Separation and Identification by Experimental Methods

While previous strigolactone syntheses were shown to be (*E*)-selective,[7] the alkylation conditions used in the report of Rasmussen et al. differed significantly from those reported, and the procedures are known to be able to induce significant changes in the *E*/*Z*-selectivity upon O-alkylation of enolates.[8] An attempt was made to determine whether the isomers are (*E*)- or (*Z*)-configured based on the obtained $^1$H NMR spectra. The double bond geometry of strigolactones is primarily assigned based on NMR spectroscopy, using the anisotropic effect induced by the ester functionality on the enolic proton. This assignment is heavily based on the early reports of MacAlpine and Raphael,[9] describing the photochemical isomerisation of (*E*)-**6** to (*Z*)-**6** (Figure 2) and the effect on the enol ether proton shift (7.38 and 6.80 ppm, respectively). Although the absolute configuration of **6**, and the closely related compounds reported by Weizel,[10] was never confirmed by X-ray analysis, the chemical shift of the initially isolated conformer, claimed to be the (*E*)-isomer, correlates closely to that of other, similarly configured SLs, such as strigol **1**, GR24 **2** (Figure 1) and Nijmegen-1 **7** (Figure 2).[1,4,11]

In our case, both obtained isomers (minor: 7.87 ppm and major: 8.16 ppm) are seemingly more consistent with the (*Z*)-configuration. However, it should be noted that the observed $^1$H NMR shift values are relatively high. The closest reported (*Z*)-configured analogue displays a shift of 7.6 ppm (**8**; Figure 2).[12] Whereas some similar (*E*)-configured compounds (for example compound **9**, Figure 2) have been reported in patents,[13] the NMR spectroscopic data for these compounds were either not reported, or the double bond geometry assignment was ambiguous. Furthermore, recent reports have shown that strigolactones of unnatural configuration may also display high shifts for the enol ether proton. Peagol (**10**; Figure 2), for example, was reported with a chemical shift of 7.59 ppm.[14] NMR-based determination depends on anisotropic effects resulting from the ester group; however, in SL analogue **3**, similar anisotropic effects may emerge from both the aromatic isoindole group and the nitrile. Therefore, the use of chemical shift and simple comparison with reported data is not conclusive. Previously reported NOESY experiments on the obtained mixture delivered no indication of the (*E*)- or (*Z*)-geometry.[5] During further NOESY experiments under nonstandard conditions, a small (–1.2%) but inconsistent effect was observed between the ethoxy $CH_3$ and the enol ether proton of the minor isomer at mixing times of three seconds (see the Supporting Information).

As previously reported, standard preparative chromatographic methods could not be used to separate the isomers.[5] However, the isomers did elute as two clearly separated peaks upon HPLC analysis (major/minor ratio 60:40, 25 °C, $CH_3CN/H_2O$, by UV-integration at 230 nm). Therefore, a sample of the product was submitted to semipreparative HPLC. Although the isomers were not completely separated, the UV-chromatogram showed a clear enrichment of both isomers (Figure 3). Surprisingly, however, after evaporation of the eluent, NMR analysis of both fractions showed a restored isomeric ratio (major/minor ratio 55:45, 20 °C, $CDCl_3$, by $^1$H NMR integration of the enol ether proton), which clearly indicated the interconversion of the isomers.

Given that removal of the water/acetonitrile eluent mixture required long evaporation times or slight heating (ca. 50 °C), isomerisation prior to $^1$H NMR analysis was very difficult to avoid. Therefore, we opted to directly monitor the isomerisation process by chromatographic methods. The enriched fractions collected from the semipreparative HPLC run were submitted to standard HPLC analysis at regular time intervals without evaporation. As shown in

  

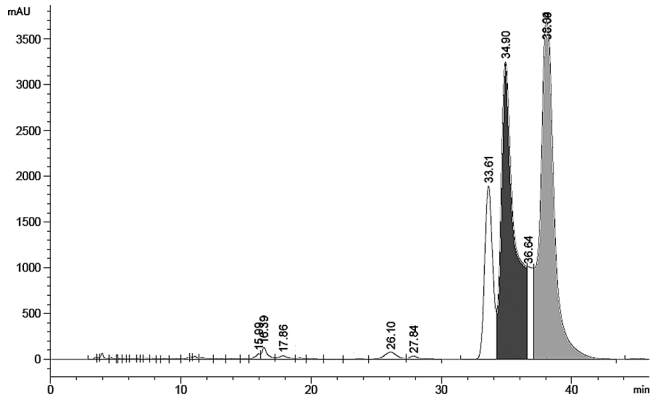


Figure 3. Fractionation of the CISA-1 isomers by semipreparative HPLC.

Figure 4, at ambient temperatures, the 60:40 equilibrium ratio was restored within 4 to 6 h.

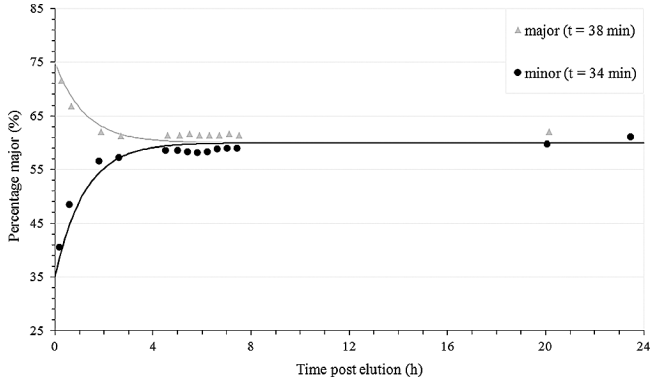


Figure 4. Evolution of the composition of the fractions collected from semipreparative HPLC (see Figure 3); (triangles) major enriched fraction collected after 38.09 min; (circles) minor enriched fraction collected after 34.90 min.

These observations clearly indicate that the obtained mixture is at equilibrium; however, the true nature of the isomers remains unclear. Initially, an *E*/*Z*-mixture of the formed enol ether was considered,[5] however, because the isomers interconvert at room temperature, rotation around the double bond is not likely. Alternatively, hindered rotation about the C–N bond between the isoindole ring and the plane of the enol ether (as shown in Figure 1) could result in two atropisomers of either the (*E*)- or (*Z*)-configuration, which may interconvert at room temperature. The exact nature of the CISA-1 isomers and their interconversion is investigated further in the following section.

## (*E*)- and (*Z*)-Isomers and Barriers for Their Interconversion Determined by Computational Methods

To determine whether CISA-1 isomers are (*E*)- or (*Z*)-configured and to understand the mechanism by which they interconvert, the stability of the isomers and their interconversion barriers were investigated with computational methods. Furthermore, computational $^1$H NMR chemical shifts for the (*E*)- and (*Z*)-isomers were compared with experimental data to assign the (*E*)- or (*Z*)-nature of the isomers.

All plausible isomers of SL analogue **3**, including diastereomers resulting from the chiral centre in the lactone ring, are shown in Figure 5. There are four enantiomeric pairs: (*E*)-*P*-*R* and (*E*)-*M*-*S*, (*E*)-*M*-*R* and (*E*)-*P*-*S*, (*Z*)-*P*-*R* and (*Z*)-*M*-*S*, and (*Z*)-*M*-*R* and (*Z*)-*P*-*S*. Since enantiomers can only be separated by the use of a chiral agent, the experimentally observed isomers are, in fact, two enantiomeric pairs.

Due to the presence of ten single bonds in CISA-1, the conformational space for each isomer is quite large. However, an initial conformational search on the butenyl-, ester- and enol ether groups gave rise to a rational and systematic choice of 24 conformers for each isomer. These conformers were optimised with B3LYP and M06-2X and for each isomer, the energies of the unique conformers were Boltzmann weighted. Relative Gibbs free energies and representative low energy M06-2X structures for the SL analogue **3** isomers are shown in Table 1 and Figure 6, respectively. For both methods, the (*Z*)-isomers are clearly more stable than the (*E*)-isomers (2.61–4.51 and 1.44–3.90 kcal/mol for

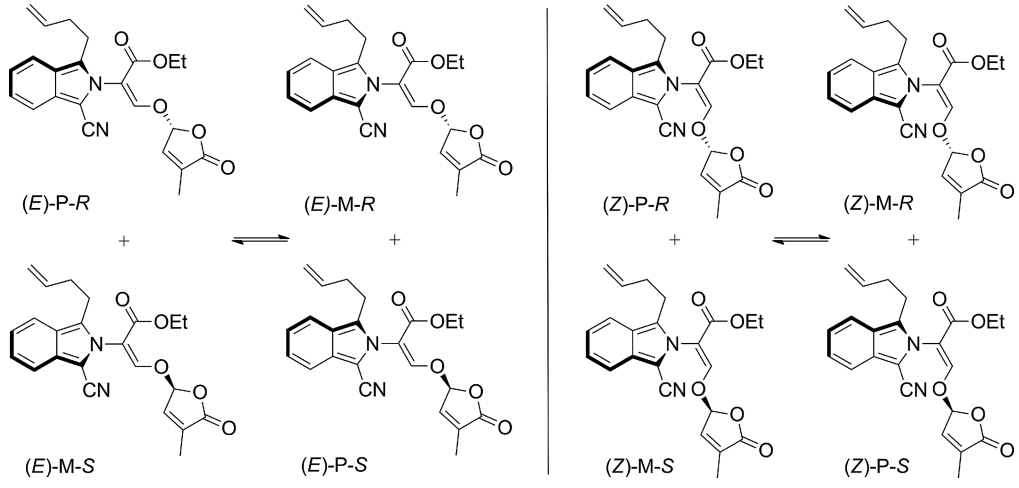


Figure 5. Plausible isomers of SL analogue **3**.

  

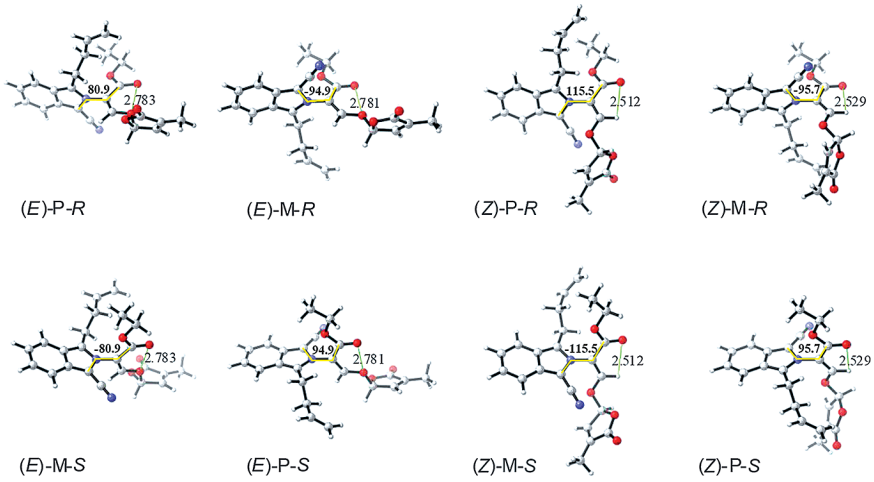


Figure 6. Representative low-energy structures of SL analogue **3** isomers [PCM ($\varepsilon$ = 7.4257) M06-2X/6-31+G(d,p)]. Some critical distances (green [Å]) and dihadral angles (yellow, degrees) are shown.

B3LYP and M06-2X calculations, respectively). This is understandable because the planarity of the enol ether and the ester causes repulsion between two oxygen atoms in the (*E*)-isomers [O–O distances are 2.68–2.79 Å (M06-2X)]. Furthermore, in the (*Z*)-configuration the alkene hydrogen atom of the enol ether is somewhat stabilised by an oxygen atom of the ester [H–O distances are 2.39–2.53 Å (M06-2X)].

Detailed investigation of the isomer stabilities clearly shows that the (*Z*)-isomers of SL analogue **3** are more stable than the (*E*)-isomers. However, this is not conclusive enough to deduce that the experimentally obtained isomers are (*Z*)-configured.

Table 1. Boltzmann weighted relative Gibbs free energies [kcal/mol] of SL analogue **3** isomers.[a]

| | (*E*)-*P*-*R*/ (*E*)-*M*-*S* | (*E*)-*M*-*R*/ (*E*)-*P*-*S* | (*Z*)-*P*-*R*/ (*Z*)-*M*-*S* | (*Z*)-*M*-*R*/ (*Z*)-*P*-*S* |
|---|---|---|---|---|
| B3LYP/6-31+G(d) | 3.50 | 4.51 | 0.89 | 0.00 |
| M06-2X/6-31+G(d,p) | 2.54 | 3.90 | 1.10 | 0.00 |

[a] PCM ($\varepsilon$ = 7.4257).

The interconversion between the *P* and *M* atropisomers was studied to check whether the activation barriers could be readily overcome at room temperature. Hindered rotation about the C–N bond between the isoindole ring, and

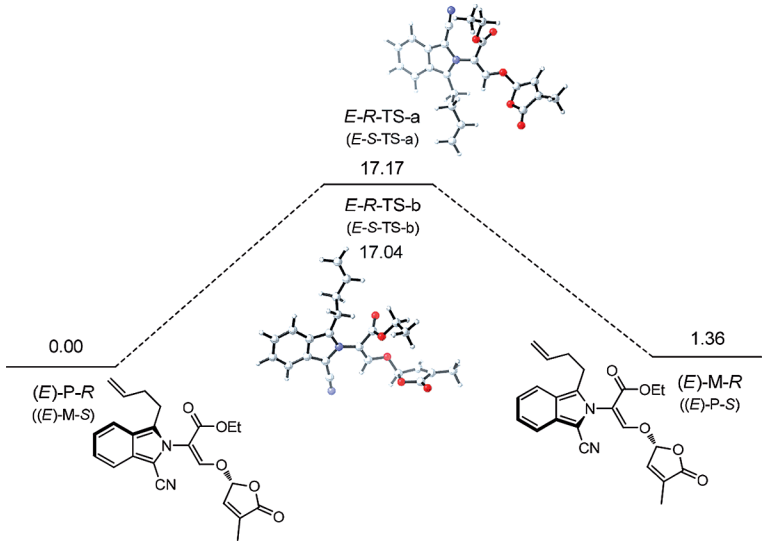


Figure 7. Gibbs free energy profile [kcal/mol] for the interconversion between SL analogue **3** isomers (*E*)-*P*-*R* and (*E*)-*M*-*R* [and (*E*)-*M*-*S* and (*E*)-*P*-*S*] [PCM ($\varepsilon$ = 7.4257) M06-2X/6-31+G(d,p)].

  

Table 2. Gibbs free activation energies $\Delta G$ [kcal/mol] and calculated half-life times[a] (h) for the interconversion between SL analogue **3** atropisomers [PCM ($\varepsilon$ = 7.4257) M06-2X/6-31+G(d,p)].

| | $\Delta G_{TS-a}$ [kcal/mol] | $t_{1/2,TS-a}$ [h] | $\Delta G_{TS-b}$ [kcal/mol] | $t_{1/2,TS-b}$ [h] |
|---|---|---|---|---|
| (*E*)-*P*-*R* to (*E*)-*M*-*R*/ (*E*)-*M*-*S* to (*E*)-*P*-*S* | 17.17 | $1.20\times10^{-4}$ [$2.13\times10^{-6}$ to $6.78\times10^{-3}$] | 17.04 | $9.64\times10^{-5}$ [$1.71\times10^{-6}$ to $5.44\times10^{-3}$] |
| (*E*)-*M*-*R* to (*E*)-*P*-*R*/ (*E*)-*P*-*S* to (*E*)-*M*-*S* | 15.81 | $1.21\times10^{-5}$ [$2.13\times10^{-7}$ to $6.81\times10^{-4}$] | 15.68 | $9.67\times10^{-6}$ [$1.71\times10^{-7}$ to $5.46\times10^{-4}$] |
| (*Z*)-*P*-*R* to (*Z*)-*M*-*R*/ (*Z*)-*M*-*S* to (*Z*)-*P*-*S* | 23.30 | 3.72 [$6.58\times10^{-2}$ to $2.10\times10^{2}$] | 24.05 | 13.26 [$2.35\times10^{-1}$ to $7.49\times10^{2}$] |
| (*Z*)-*M*-*R* to (*Z*)-*P*-*R*/ (*Z*)-*P*-*S* to (*Z*)-*M*-*S* | 24.40 | 23.85 [$4.22\times10^{-1}$ to $1.35\times10^{3}$] | 25.15 | 85.10 [1.51 to $4.81\times10^{3}$] |

[a] Minimum and maximum values, based on a estimated margin of error of 10 kJ/mol (2.38 kcal) on the Gibbs free activation energies, in squared brackets. An energy difference with an error of ±10 kJ/mol is said to be within chemical accuracy, although in recent years there have been some efforts to get to 5 kJ/mol.[15]

the plane of the enol ether is possible in two directions. The rotation whereby the alkenyl group passes the enol ether gives rise to one transition state (TS-a) and the rotation whereby the alkenyl group passes the ester gives rise to a second (TS-b). The Gibbs free energy profiles (M06-2X) for the interconversion between isomers (*E*)-*P*-*R* and (*E*)-*M*-*R* (and their enantiomers) and (*Z*)-*P*-*R* and (*Z*)-*M*-*R* (and their enantiomers) by rotation about the C–N bond are shown in Figure 7 and Figure 8, respectively. Gibbs free activation energies $\Delta G$ and calculated half-lives for the interconversion between the isomers are shown in Table 2.

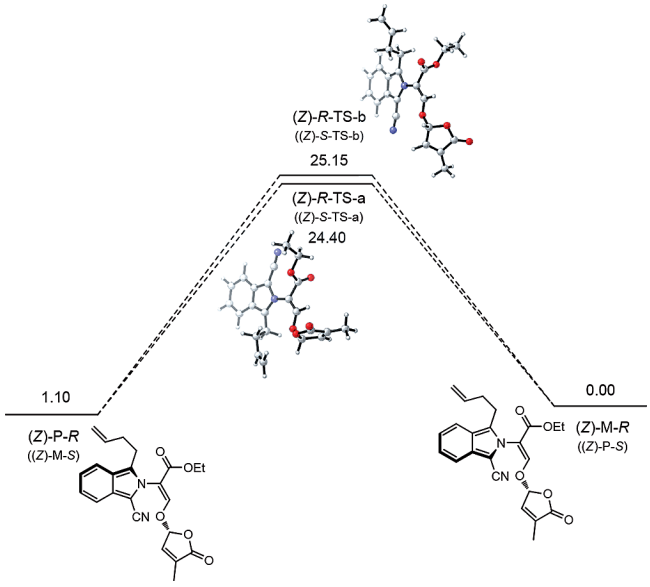


Figure 8. Gibbs free energy profile [kcal/mol] for the interconversion between SL analogue isomers (*Z*)-*P*-*R* and (*Z*)-*M*-*R* [and (*Z*)-*M*-*S* and (*Z*)-*P*-*S*] [PCM ($\varepsilon$ = 7.4257) M06-2X/6-31+G(d,p)].

The activation barriers for interconversion between the (*E*)-isomers are remarkably lower than the activation barriers for interconversion between the (*Z*)-isomers (15.68–17.17 and 23.30–25.15 kcal/mol, respectively), which is understandable because there is less steric hindrance when the lactone ring is orientated away from the rotational bond. These calculated activation barriers for interconversion between the (*E*)-isomers give rise to half-lives of less than a second, whereas the activation barriers for interconversion between the (*Z*)-isomers give rise to half-lives of several (tens of) hours (Table 2). The rapid interconversion between (*E*)-isomers would lead to very fast reinstatement of the original isomer ratio and chromatographic separation or enrichment of the isomers would not be feasible. This finding also seems to further validate the conclusion that the observed isomers are most likely the more stable (*Z*)-isomers. However, the relatively large margin of error on the calculated half-lives indicates that these results are insufficient to obtain a definitive answer.

For completeness, *E*/*Z*-isomerisation was also studied. Gibbs free activation energies $\Delta G$ were found to be more than 50 kcal/mol (M06-2X), confirming that rotation around the double bond will not take place at room temperature. The Gibbs free energy profiles for the interconversion can be found in the Supporting Information.

## $^1$H NMR Chemical Shift Calculations

As previously mentioned, experimental NMR spectroscopy was inconclusive in unambiguously identifying whether the obtained isomers were (*E*)- or (*Z*)-configured. Computational $^1$H NMR chemical shifts for the enolic proton (C=CHO) of the CISA-1 (*E*)- and (*Z*)-isomers were compared with the experimental $^1$H NMR spectroscopic data.

Calculation of NMR shifts has played a key role in the structure assignment and reassignment of complex natural products as well as products obtained through synthetic chemistry, and the approach has become a reliable tool for computational and synthetic organic chemists over the past decade.[16] Although it is often difficult to assign every peak in an experimental spectrum to the corresponding nuclei, there is a clear correspondence between the computed chemical shifts and the associated nuclei. Furthermore, good quality NMR calculations can usually be used to distinguish between closely related structures, such as diastereomers, when experimental spectra alone are not enough to give unambiguous proof of the precise stereochemistry. DP4 statistical analysis can help to assign structure and stereochemistry by comparing experimental and calculated NMR spectra and calculating the probability

  

that each compound gives rise to the experimental spectrum.[17]

Based on the conformational search in the previous section, $^1$H NMR chemical shifts were calculated according to the general protocol described by Willoughby et al.[18] All conformers were reoptimised in chloroform with the same level of theory [M06-2X/6-31+G(d,p)]. For each unique conformer, NMR shielding tensors were calculated with the GAIO method at the B3LYP/6-311+G(2d,p) level of theory in chloroform. Rather than subtract the shielding tensor value of TMS from the calculated tensor values, a more reliable approach was chosen, utilising scaling parameters derived from linear regression analysis of a test set of molecules for this specific combination of functional and basis set.[16]

$\delta = \frac{\sigma - 31.9477}{-1.0767}$, with $\delta$ the chemical shift and $\sigma$ the calculated shielding tensor.

Finally, the obtained chemical shifts were Boltzmann weighted for each isomer.

The calculated and experimental $^1$H NMR chemical shift values for the enolic proton (C=CHO) of CISA-1 are shown in Table 3. The calculated chemical shifts for the minor and major (*Z*)-isomers are in very good agreement with the experimental data[5] (7.77 vs. 7.87 and 8.09 vs. 8.16 ppm for the minor and the major fractions, respectively), whereas the difference between the calculated and the experimental chemical shifts is significantly higher for the (*E*)-isomers (7.03 vs. 7.87 and 7.24 vs. 8.16 ppm for the minor and the major fractions, respectively), confirming the (*Z*)-conformation of the isomers. The mean absolute errors (MAE), which are defined as the differences between the calculated and the experimental chemical shift values averaged over the different conformers for each isomer, for the minor and the major fractions of the (*Z*)-isomers are 0.24 and 0.26 ppm, with largest absolute errors 0.35 and 0.56 ppm, respectively. Apart from the energetic considerations, the correspondence between calculated $^1$H NMR chemical shifts of the (*Z*)-isomers and the experimental values allows the experimentally observed isomers to be assigned as (*Z*)-isomers.

Table 3. Calculated and experimental $^1$H NMR chemical shifts (ppm) for the enolic proton (C=CHO) of CISA-1 [PCM ($\varepsilon$ = 4.7113) B3LYP/6-311+G(2d,p)//PCM ($\varepsilon$ = 4.7113) M06-2X/6-31+G(d,p)].[a]

| | Minor | Major |
|---|---|---|
| Calculated (*E*)-isomers | 7.03 (0.78) | 7.24 (1.06) |
| Calculated (*Z*)-isomers | 7.77 (0.24) | 8.09 (0.26) |
| Experimental[5] | 7.87 | 8.16 |

[a] MAE (mean absolute error) in parenthesis.

## Conclusions

The strigolactone analogue CISA-1 was originally isolated as a mixture of isomers. Whereas standard experimental techniques could not be used to determine the nature of the isomers, chromatographic enrichment did prove the interconversion of these isomers at room temperature, resulting in the reinstatement of the 60:40 equilibrium within a few hours, and thus excluding *E*/*Z* isomers. To identify the true nature of the isomers, their stability and the barriers for their interconversion were investigated by computational methods. The (*Z*)-isomers are clearly more stable than the (*E*)-isomers. Hindered rotation about the C–N bond between the isoindole and the enol ether results in two atropisomers *P* and *M*. The activation barriers for interconversion between the (*E*)-configured atropisomers give rise to half-lives of less than a second, whereas the activation barriers for interconversion between the (*Z*)-atropisomers give rise to half-lives of several (tens of) hours. Furthermore, calculated $^1$H NMR shift values point to the (*Z*)-isomer. Therefore, the experimentally observed isomers of CISA-1 are concluded to be the more stable (*Z*)-isomers, more particularly, the isomeric pairs (*Z*)-*P*-*R* and (*Z*)-*M*-*S* (minor), and *Z*-*M*-*R* and *Z*-*P*-*S* (major).

Over the last year, several fluorescent strigolactones containing bulky aromatic side chains have been developed.[19] While this is the first report on the occurrence of atropisomers, and the rate of interconversion for this specific derivative is sufficiently high to warrant full bioavailability, it must be taken into account during the development of new analogues. As the steric bulk increases, the C–N rotation may slow down significantly, resulting in stable atropisomers. These atropisomers are expected to have different bioactivity.

## Experimental Section

**Experimental Techniques:** Preparative HPLC separations were carried out with an Agilent 1100 series HPLC, using a ZORBAX XDB-C18 column (21.2 × 150 mm, 5 μm), $CH_3CN/H_2O$ from 0:100 to 55:45 over 50 min. Nonstandard NOESY experiments were performed with increased mixing times (3 s) with a Bruker Avance III Nanobay 400 MHz spectrometer at room temperature.

**Computational Methodology:** Two levels of theory, B3LYP/6-31+G(d,p)[20] and M06-2X/6-31+G(d,p),[21] were used for geometry optimisations. Preliminary B3LYP energies were improved by means of geometry optimisations with the M06-2X functional, which is able to account for noncovalent interactions and has been successfully used to describe thermochemistry. More specifically, intramolecular dispersion effects have to be taken into account for the large molecules studied herein.[22] A conformational analysis was performed on all isomers and transition states.[23] Stationary points were characterised as minima (ground states) or first-order saddle points (transition states) through frequency calculations. IRC (intrinsic reaction coordinate) calculations[24] followed by geometry optimisations were used to verify the corresponding reactant and product complexes. Since the reactions under study take place in tetrahydrofuran ($\varepsilon$ = 7.4257), which cannot form hydrogen bonds with the substrate, the solvent environment was taken into account by means of a polarisable continuum model (PCM).[25] $^1$H NMR calculations were carried out with the GAIO (gauge invariant atomic orbitals) method[26] at the B3LYP/6-311+G(2d,p)//M06-2X/6-31+G(d,p) level of theory in chloroform ($\varepsilon$ = 4.7113), according to the general procedure described by Willoughby et al.[18] All

  

computations were performed with the Gaussian 09 program package.[27]

**Supporting information** (see footnote on the first page of this article): Cartesian coordinates, energies, imaginary and low frequencies of the optimised geometries [PCM ($\varepsilon$ = 7.4257) M06-2X/6-31+G(d,p)]; NOESY and HPLC spectra

## Acknowledgments

The Fund for Scientific Research, Flanders (FWO Vlaanderen), the Research Board of Ghent University and the Belgium Federal Government via the Interuniversity Attraction Poles Scheme 7/05 are gratefully acknowledged for financial support. The computational resources used in this work were provided by Stevin Supercomputer Infrastructure Ghent University (Belgium). V. A. acknowledges support by the State Planning Organization−Turkey (project number DPT-2009K120520).

[1] C. E. Cook, L. P. Whichard, B. Turner, M. E. Wall, G. H. Egley, *Science* **1966**, *154*, 1189.
[2] B. Zwanenburg, T. Pospisil, *Mol. Plant* **2013**, *6*, 38; C. Ruyter-Spira, S. Al-Babili, S. Van der Krol, H. Bouwmeester, *Trends Plant Sci.* **2013**, *18*, 72; P. B. Brewer, H. Koltai, C. A. Beveridge, *Mol. Plant* **2013**, *6*, 18; Y. Seto, H. Kameoka, S. Yamaguchi, J. Kyozuka, *Plant Cell Physiol.* **2012**, *53*, 1843; X. Xie, K. Yoneyama, K. Yoneyama, *Annu. Rev. Plant Physiol.* **2010**, *48*, 93.
[3] D. Sato, A. A. Awad, Y. Takeuchi, K. Yoneyama, *Biosci. Biotechnol. Biochem.* **2005**, *69*, 98.
[4] A. W. Johnson, G. Roseberry, C. Parker, *Weed Res.* **1976**, *16*, 223; A. W. Johnson, G. Gowda, A. Hassanali, J. Knox, S. Monaco, Z. Razawi, G. Roseberry, *J. Chem. Soc. Perkin Trans. 1* **1981**, 1734; E. M. Mangnus, F. J. Dommerholt, R. L. P. de Jong, B. Zwanenburg, *J. Agric. Food Chem.* **1992**, *40*, 1230; W. J. F. Thuring, G. H. L. Nefkens, B. Zwanenburg, *J. Agric. Food Chem.* **1997**, *45*, 2278.
[5] A. Rasmussen, T. S. A. Heugebaert, C. Matthys, R. Van Deun, F.-D. Boyer, S. Goormachtig, C. V. Stevens, D. Geelen, *Mol. Plant* **2013**, *6*, 100; T. S. A. Heugebaert, C. V. Stevens, *Org. Lett.* **2009**, *11*, 5018.
[6] F.-D. Boyer, A. De Saint Germain, J.-B. Pouvreau, G. Clavé, J.-P. Pilot, A. Roux, A. Rasmussen, S. Depuydt, D. Lauressergues, N. Frei dit Frey, T. S. A. Heugebaert, C. V. Stevens, D. Geelen, S. Goormachtig, C. Rameau, *Mol. Plant* **2014**, *7*, 675.
[7] Please note that IUPAC nomenclature prescribes that the configuration corresponding to the (*E*)-configuration of natural strigolactones and previously reported analogues, be named the (*Z*)-configuration of CISA-1, this due to the presence of the isoindole nitrogen.
[8] E. V. Dehmlov, M. Kaiser, J. Bollhöfer, *New J. Chem.* **2001**, *25*, 588.
[9] C. E. Cook, L. P. Whichard, M. Wall, E. G. H. Egley, P. Coggon, P. A. Luhan, A. T. McPhail, *J. Am. Chem. Soc.* **1972**, *94*, 6198; G. A. MacAlpine, R. A. Raphael, A. Shaw, A. W. Taylor, H.-J. Wild, *J. Chem. Soc., Chem. Commun.* **1974**, 834; G. A. MacAlpine, R. A. Raphael, A. Shaw, A. W. Taylor, H.-J. Wild, *J. Chem. Soc. Perkin Trans. 1* **1976**, 410.
[10] S. Röhrig, L. Hennig, M. Findeisen, P. Weisel, *Tetrahedron* **1998**, *54*, 3413.
[11] G. H. L. Nefkens, W. J. F. Thuring, M. F. M. Beenakkers, B. Zwanenburg, *J. Agric. Food Chem.* **1997**, *45*, 2273.
[12] G. Camaggi, L. Filippini, M. Gusmeroli, G. Meazza, R. Riva, G. Zanardi, C. Garavaglia, L. Mirenna, Can. Pat. Appl. CA 2088870 A1, **1993** (CAN120:191708); P. DeFraine, B. K. Snell, J. M. Clough, V. M. Anthony, K. Beautement, Eur. Pat. Appl. EP 206523 A1, **1986** (CAN106:98100).
[13] A. Klausener, D. Berg, T. Seitz, W. Brandes, S. Dutzmann, G. Haenssler, U. Wachendorff-Neumann, Ger. Offen. DE 3939238 A1, **1991** (CAN115:159128); R. P. Warrington, G. Ramsay, N. R. Bird, Eur. Pat. Appl. EP 415569 A2, **1991** (CAN115:87516); J. M. Clough, C. R. A. Godfrey, P. J. De Fraine, B. K. Snell, Eur. Pat. Appl. EP 273572 A2, **1988** (CAN109:190240).
[14] A. Evidente, M. Fernández-Aparicio, A. Cimmino, D. Rubiales, A. Andolfi, A. Motta, *Tetrahedron Lett.* **2009**, *50*, 6955.
[15] E. G. Lewars, *Computational Chemistry*, Springer, Netherlands, **2011**.
[16] M. W. Lodewyk, M. R. Siebert, D. J. Tantillo, *Chem. Rev.* **2012**, *112*, 1839; and references cited therein.
[17] S. G. Smith, J. M. Goodman, *J. Am. Chem. Soc.* **2010**, *132*, 12946.
[18] P. H. Willoughby, M. J. Jansma, T. R. Hoye, *Nat. Protoc.* **2014**, *9*, 643.
[19] C. Prandi, E. G. Occhiato, S. Tabasso, P. Bonfante, M. Novero, D. Scarpi, M. E. Bova, I. Miletto, *Eur. J. Org. Chem.* **2011**, 3781; C. Bhattacharya, P. Bonfante, A. Deagostino, Y. Kapulnik, P. Larini, E. G. Occhiato, C. Prandi, P. Venturello, *Org. Biomol. Chem.* **2009**, *7*, 3413.
[20] C. T. Lee, W. T. Yang, R. G. Parr, *Phys. Rev. B* **1988**, *37*, 785; A. D. Becke, *J. Chem. Phys.* **1993**, *98*, 5648.
[21] Y. Zhao, D. G. Truhlar, *Theor. Chem. Acc.* **2008**, *120*, 215.
[22] S. Catak, K. Hemelsoet, L. Hermosilla, M. Waroquier, V. Van Speybroeck, *Chem. Eur. J.* **2011**, *17*, 12027; A. De Blieck, S. Catak, W. Debrouwer, J. Drabowicz, K. Hemelsoet, T. Verstraelen, M. Waroquier, V. Van Speybroeck, C. Stevens, *Eur. J. Org. Chem.* **2013**, 1058.
[23] Conformational analysis was done manually: 6 × 3 × 3 conformations for the butenyl group, 2 × 3 × 3 conformations for the ester group and 3 × 3 conformations for the enol ether group were explored. No specific software was employed.
[24] K. Fukui, *Acc. Chem. Res.* **1981**, *14*, 36.
[25] C. J. Cramer, D. G. Truhlar, *Solvent Effects and Chemical Reactivity*, Kluwer, Dordrecht, The Netherlands, **1996**; V. Barone, M. Cossi, *J. Phys. Chem. A* **1998**, *102*, 1995; M. Cossi, N. Rega, G. Scalmani, V. J. Barone, *Comput. Chem.* **2003**, *24*, 669.
[26] F. London, *J. Phys. Radium* **1937**, *8*, 397; R. Ditchfield, *J. Chem. Phys.* **1972**, *56*, 5688; K. Wolinski, J. F. Hinton, P. Pulay, *J. Am. Chem. Soc.* **1990**, *112*, 8251.
[27] M. J. Frisch, G. W. Trucks, H. B. Schlegel, G. E. Scuseria, M. A. Robb, J. R. Cheeseman, G. Scalmani, V. Barone, B. Mennucci, G. A. Petersson, H. Nakatsuji, M. Caricato, X. Li, H. P. Hratchian, A. F. Izmaylov, J. Bloino, G. Zheng, J. L. Sonnenberg, M. Hada, M. Ehara, K. Toyota, R. Fukuda, J. Hasegawa, M. Ishida, T. Nakajima, Y. Honda, O. Kitao, H. Nakai, T. Vreven, J. A. Montgomery Jr, J. E. Peralta, F. Ogliaro, M. Bearpark, J. J. Heyd, E. Brothers, K. N. Kudin, V. N. Staroverov, R. Kobayashi, J. Normand, K. Raghavachari, A. Rendell, J. C. Burant, S. S. Iyengar, J. Tomasi, M. Cossi, N. Rega, J. M. Millam, M. Klene, J. E. Knox, J. B. Cross, V. Bakken, C. Adamo, J. Jaramillo, R. Gomperts, R. E. Stratmann, O. Yazyev, A. J. Austin, R. Cammi, C. Pomelli, J. W. Ochterski, R. L. Martin, K. Morokuma, V. G. Zakrzewski, G. A. Voth, P. Salvador, J. J. Dannenberg, S. Dapprich, A. D. Daniels, Ö. Farkas, J. B. Foresman, J. V. Ortiz, J. Cioslowski, D. J. Fox, *Gaussian 09*, revision B.01, Gaussian, Inc., Wallingford CT, **2009**.

Received: November 10, 2014
Published Online: ■

  

**Atropisomerism**

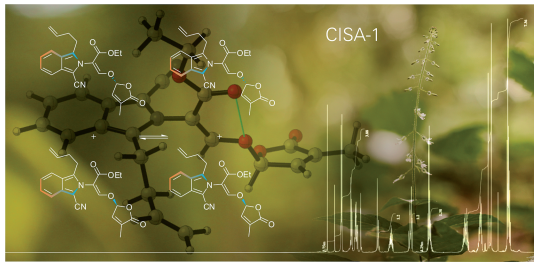


The occurrence of atropisomers among strigolactone analogues is reported for the first time. While the rate of interconversion for this specific derivative is sufficiently high to warrant full bioavailability, these findings are of high importance for the development of new analogues that could lead to stable atropisomers with different bioactivity.



**Keywords:** Atropisomerism / Lactones / Conformation analysis / Configuration determination / Density functional calculations

  